Send Orders for Reprints to reprints@benthamscience.ae

300 *Current Analytical Chemistry*, 2015, *11*, 300-306

A Derivative Method with Free Radical Oxidation to Predict Resveratrol Metabolites by Tandem Mass Spectrometry

Wangta Liu[1], Yow-Ling Shiue[2], Yi-Reng Lin[3], Hugo You-Hsien Lin[4,5,6] and Shih-Shin Liang*[1,2,7]

[1]Department of Biotechnology, Kaohsiung Medical University, Kaohsiung, Taiwan; [2]Institute of Biomedical Science, National Sun Yat-Sen University, Kaohsiung, Taiwan; [3]Department of Biotechnology, Fooyin University, Kaohsiung, Taiwan; [4]Graduate Institute of Medicine, Kaohsiung Medical University, Kaohsiung, Taiwan; [5]Division of Nephrology, Department of Internal Medicine, Kaohsiung Medical University Hospital, Kaohsiung Medical University, Kaohsiung, Taiwan; [6]Department of Internal Medicine, Kaohsiung Municipal Ta-Tung Hospital, Kaohsiung Medical University, Kaohsiung, Taiwan; [7]Center for Resources, Research and Development, Kaohsiung Medical University, Kaohsiung, Taiwan

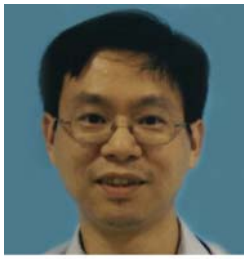

Shih-Shin Liang

Abstract: In this study, we demonstrated an oxidative method with free radical to generate 3,5,4′-trihydroxy-*trans*-stilbene (*trans*-resveratrol) metabolites and detect sequentially by an autosampler coupling with liquid chromatography electrospray ionization tandem mass spectrometer (LC-ESI–MS/MS). In this oxidative method, the free radical initiator, ammonium persulfate (APS), was placed in a sample bottle containing resveratrol to produce oxidative derivatives, and the reaction progress was tracked by autosampler sequencing. Resveratrol, a natural product with purported cancer preventative qualities, produces metabolites including dihydroresveratrol, 3,4′-dihydroxy-*trans*-stilbene, lunularin, resveratrol monosulfate, and dihydroresveratrol monosulfate by free radical oxidation. Using APS free radical, the concentrations of resveratrol derivatives differ as a function of time. Besides simple, convenient and time- and labor saving, the advantages of free radical oxidative method of its *in situ* generation of oxidative derivatives followed by LC-ESI–MS/MS can be utilized to evaluate different metabolites in various conditions.

Keywords: Free radical, metabolite, resveratrol, ammonium persulfate (APS), liquid chromatography tandem mass spectrometry (LC–MS/MS), multiple reaction monitoring (MRM).

1. INTRODUCTION

In the last decades, metabolomics has developed at an amazing rate in the –omics field. At an early stage of development in the research of metabolic derivatives, biological generation method can be used; specifically, human and rat liver microsomes (HLMs & RLMs) were processed to investigate metabolites with specific cytochrome P450 (CYP450) activity [1-4]. However, metabolites studied by HLM and RLM methods are expensive, time consuming, and labor intensive. Besides, under different conditions and extraction times, the results of HLM or RLM treatments will display different profiles in HLM and RLM metabolites [1].

In addition, electrochemical methods for producing metabolites, such as cyclic voltammetry (CV) use various buffer solutions, probes, and voltage values to generate oxidative and reductive derivatives. For example, metabolic or oxidative products of uric acid were detected by C-60-modified glassy carbon electrodes [5], and multi-walled carbon-nanotube-modified carbon-ceramic electrodes [6]. In another studies, electrochemical oxidation of adenosine and guanosine-5′-triphosphate was investigated by glassy carbon and pyrolytic graphite electrodes [7, 8]. Additionally, DNA and DNA-related biological researches including DNA damage were demonstrated [9-11]. However, CV is an off-line technique and is incompatible with tandem MS. Furthermore, researchers have to contend with electrode aging, probes' activity and stability loss over time. The results of CV technique cannot directly show compound antioxidant capacities [12]. Consequently, there was a novel method which was integrated Fenton reaction to generate free radical and CV to demonstrate mimic drug metabolites in phase I period [13, 14].

Nevertheless, for studying well-known metabolites, it is convenient to utilize the detection mode multiple reaction monitoring (MRM) by tandem mass spectrometry. In the previous studies, electrochemical cells (EC) coupled with electrospray ionization–tandem mass spectrometer (EC-ESI–MS/MS) can be used as powerful online instruments for oxidative derivative detection and prediction of metabolites [15-19]. In recent years, the application of EC-ESI–MS/MS systems has been extended to include separation apparatus such as liquid chromatograph (LC) to generate EC/LC-ESI–MS/MS systems [13, 14]. Using this type of instrument, tetrazepam metabolism has been investigated by comparing *in vivo* and *in vitro* methods [18, 19]. Similar EC/LC–

*Address correspondence to this author at the Department of Biotechnology, Kaohsiung Medical University, P.O. Box: 80708 Kaohsiung, Taiwan; Tel/Fax: +886-7-3121101-2153, +886-7-312-5339;
E-mail: liang0615@kmu.edu.tw

1875-6727/15 $58.00+.00

MS/MS methods have been developed for many applications including protein adduct formation by thimerosal with human serum albumin and β-lactoglobulin A [20], protein adduct formation of aniline [21], nucleotide oxidative products generation and identification [22], and protein/peptide disulfide bond conformation by tracking electrolytic cleavage [23].

In this study, we generated free radical persulfate from ammonium persulfate (APS) to demonstrate the oxidative derivatives and to predict the metabolites of resveratrol. Without CV and EC supporting, the results in metabolites of resveratrol could be shown in MS profiles. Comparison with previous studies on the metabolism of resveratrol [24, 25], we monitored the production of dihydroresveratrol, 3,4′-dihydroxy-*trans*-stilbene, lunularin, resveratrol monosulfate, and dihydroresveratrol monosulfate. By free radical oxidative method coupled with LC and tandem MS, we created an online sequentially analytical system capable of following metabolic progression. The APS oxidation method is based on a previous study that utilized Fenton reactions to demonstrate the oxidative derivatives of nicotine [26]. Because of its online, sequential nature, this method has several advantages, such as it saves time as well as avoids electrode contamination and flow cell cracking (max. pressure: 40 psi, Antec Leyden, Zoeterwoude, The Netherlands). Another important advantage is that this sequential analysis can identify the changes in oxidative derivatives over time. Based on the results, we can utilize this method to predict the production of metabolic derivatives.

In this paper, we took resveratrol (3,5,4′-trihydroxy-*trans*-stilbene, Res) as a model to demonstrate free radical oxidative method. Resveratrol is a phytophenol being found in natural foods including grapes, peanuts, and berries [27]. Resveratrol is reported to possess multiple functions such as lifespan extension [28], antioxidant effects [29], anti-inflammatory effects [30, 31], cardiovascular protective effects [32, 33], cancer prevention, and therapeutic effects [34, 35]. *trans*-Resveratrol, as a phytophenolic compound, has been recognized in intracellular forms by metabolic enzymes [25]. However, it is unclear whether it is resveratrol or one of its metabolites that produce these effects [36]. Based on these factors, we selected resveratrol as a model to evaluate free radical method by APS and compare with previous studies [24, 25]. The free radical oxidative method is different from sulfotransferase catalyzing resveratrol into related monosulfate compounds. However, metabolites can be generated and detected by utilizing suitable reactive chemical or buffer conditions.

2. MATERIAL AND METHOD

2.1. Chemicals

The chemical reagents including formic acid (FA, ACS reagent, ≥96% to volume), *trans*-resveratrol, and APS were obtained from Sigma-Aldrich (St. Louis, MO, USA). Methanol (MeOH) and acetonitrile (MeCN, LC-MS grade) were purchased from J. T. Baker (Phillipsburg, NJ, USA). Deionized water was produced by a Milli-Q system with 18.2 MΩ cm resistivity at 25 °C (Millipore, Bedford, MA).

2.2. Production of Resveratrol Metabolites with APS Free Radicals in MS Scanning Mode

APS (10% to volume) was prepared in a water solution, and resveratrol was dissolved in methanol to obtain a 10 mM resveratrol alcohol solution. The experimental solution consisted of 1764 μL of 0.1% FA (by volume), 18 μL of 10 mM resveratrol, and 18 μL of a 10% APS to finally generate a solution containing 0.1% APS (by volume) and 100 μM resveratrol. APS in solution served as a catalyst and an oxidant in these experiments. The gradient in the separation system was set at 15 min in one experiment, and 30 experiments were conducted according to priority to the online sequential sampling schedule.

2.3. MRM transitions of Oxidative Derivatives

Resveratrol oxidative derivatives can be sequentially monitored via continuous sampling. The MRM scanning mode focuses on precursor ions (*m/z* of oxidative derivatives) and product ions (*m/z* of fragmented ions) with respective MRM transitions shown in Table **1**.

2.4. Instruments

The separation system was an ultrahigh-pressure liquid chromatograph (UHPLC, Acella 1250 UHPLC, Thermo Fisher Scientific Inc., Waltham, MA, USA) coupled with ESI–MS/MS (Thermo Finnigan TSQ Quantum Ultra Mass Spectrometer Analytic System, Thermo Fisher Scientific

Table 1. Predictive metabolic derivatives of resveratrol by free radical oxidation-ESI–MS/MS. Molecular formula, molecular weight, and *m/z* of parent ion and daughter ions are listed.

Name	Molecular Formula	Mw (Da)	Precursor ion#	Product ions
trans-Resveratrol	$C_{14}H_{12}O_3$	228.24	227	143, 185
Dihydroresveratrol	$C_{14}H_{14}O_3$	230.26	229	81*, 122*, 123*, 144
3,4′-Dihydroxy-*trans*-stilbene	$C_{14}H_{12}O_2$	212.24	211	115, 143*, 169
Lunularin	$C_{14}H_{14}O_2$	214.26	213	106, 107*
Resveratrol monosulfate	$C_{14}H_{12}O_6S$	308.31	307	201, 243
Dihydroresveratrol monosulfate	$C_{14}H_{12}O_6S$	310.32	309	201, 243

Because the tandem MS method is conducted in the negative mode, the *m/z* of parent ions in each compounds decreases by one Da.
* The *m/z* of product ions is referred from a previous study [24].

Inc.). The ESI ion source was 3.0 kV in negative polarity with a tube lens offset of −188 V. Furthermore, vaporizing and capillary temperatures were set at 270 °C and 350 °C, respectively, and sheath gas and aux gas pressures were set at 35 and 10 (arbitrary units), respectively. The collision energy adjusted to 20 V with ramping 5 V, and collision pressure was set at 1.0 (arbitrary units). The full scan (FS) mode was set at *m/z* 60−350 Da in the first quadrupole chamber and unknown oxidative products with high intensities were separated, detected, and selected (intensity > 10^4) into MS collision chamber with two high-intensity signals (data dependant scan). The transferred ions passed into the collision-induced dissociation (CID) chamber for MS/MS fragmentation with a collision energy of 20 V, and further detected in the third quadrupole chamber at *m/z* 10−350 Da. The mass spectra were acquired by Xcalibur software (version 2.2, Thermo-Fisher Scientific Inc., San Jose, CA, USA). The sample containing oxidative derivatives was injected directly into the UHPLC via Acella 1250 autosampler and separated on a Shiseido HPLC CAPCELL PAK C18 MGII column (150 mm × 1.5 mm, 3.0 μm, Tokyo, Japan). The UHPLC flow rate was set at 200 μL/min (gradient pump), and the mobile phases were prepared with (A) 0.1% FA in water and (B) 0.1% FA in 100% MeCN with a linear gradient as follows: from 5% (B) in 2 min, 5%−40% (B) in 5 min, 40%−95% in 3 min, 95% (B) in 1 min, 98%−5% (B) in 0.1 min and 5% (B) in 4.9 min.

3. RESULTS AND DISCUSSION

3.1. APS Free Radical Generation for the Production of Oxidative Derivatives

A simple representation of the experimental concept is shown in Fig. (**1**). APS is able to produce two persulfate free radicals, shown in Fig. (**1A**), and oxidative derivatives can be generated in a sample bottle. The reacted oxidative products are injected into the LC–MS/MS by an autosampler for characterization of oxidative derivatives and to obtain their structural information. A simple diagram of the experimental process is shown in Fig. (**1B**).

3.2. MS and MS/MS Spectra of Resveratrol and its Oxidative Derivatives

A Structural identification of resveratrol metabolic derivatives was demonstrated by tandem MS experiments. The detailed structures of metabolic derivatives were obtained by fragmented spectra of MS/MS and compared with previous reports [24, 25]. Additionally, according to the results of the APS free radical method and previous studies, before APS addition, there was only one peak belonging to resveratrol at *m/z* 227 in the chromatogram's base peak (data shown in Fig. **2A**). However, there were some oxidative derivative peaks that were observed at *m/z* 307, 309 and 229 after APS was added. In Fig. (**2B**), the resveratrol monosulfate ion at *m/z* 307 was extracted by Xcalibur software after APS treatment, and the spectra of other oxidative derivatives were also extracted (data not shown).

The individual derivatives of fragmented ions were determined by LC–MS/MS, and the structural information belonging to oxidative derivatives was identified. Based on MS/MS spectra of Fig. (**3A**–**F**) and previous reports [24, 25], resveratrol (*m/z* 227) has fragmented ions at *m/z* 185 and 143. Additionally, the reducing form of resveratrol, dihydroresveratrol, produces characteristic MS/MS ions at *m/z* 144. However, according to the study by Bode *et al*. [24], dihydroresveratrol has other fragmented ions such as *m/z* 123, 122 and 81. In Fig. (**3C** and **D**), resveratrol monosulfate and dihydroresveratrol monosulfate have similar fragmented ions, at *m/z* 243 and 201. Finally, a hydroxyl group was subtracted by APS radicalization, and the derivatives included 3,4′-dihydroxy-*trans*-stilbene and lunularin represented by ions at *m/z* 211 and 213. The fragmented ions of 3,4′-dihydroxy-*trans*-stilbene were at *m/z* 169 and 145. Furthermore, the fragmented ions belonging to lunularin were at *m/z* 171 and 106, and the MS/MS spectra of 3,4′-dihydroxy-*trans*-stilbene and lunularin are shown in Fig. (**3E** and **F**). The final result indicates that we can generate MS and MS/MS data belonging to resveratrol and its oxidative derivatives to create an MRM method. MRM transitions are shown in Table **1**.

3.3. RESVERATROL AND ITS OXIDATIVE DERIVATIVES BASED ON SEQUENTIAL ANALYSIS BY MRM

Resveratrol and its oxidative derivatives were separated and detected by LC–MS/MS via the MRM scanning mode. According to Table **1**, the MRM transitions were set with *m/z* based on the characteristic fragmented ions belonging to resveratrol and its derivatives such as *m/z* 227 > 185 and

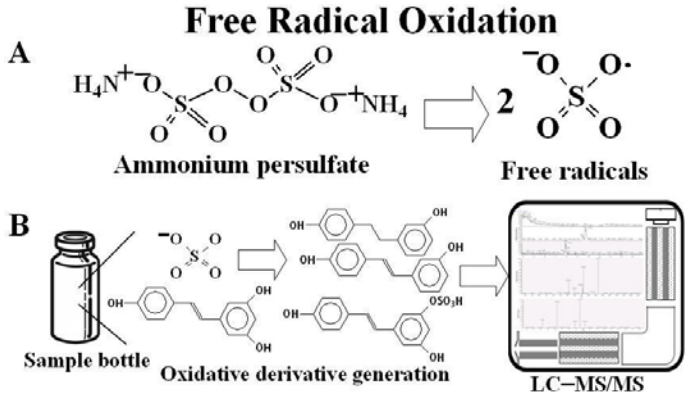

Fig. (1). Schematic representations of the free radical oxidative method; (**A**) free radicals generated by ammonium persulfate; (**B**) chemical scheme for the formation of resveratrol derivatives and the experimental detection apparatus.

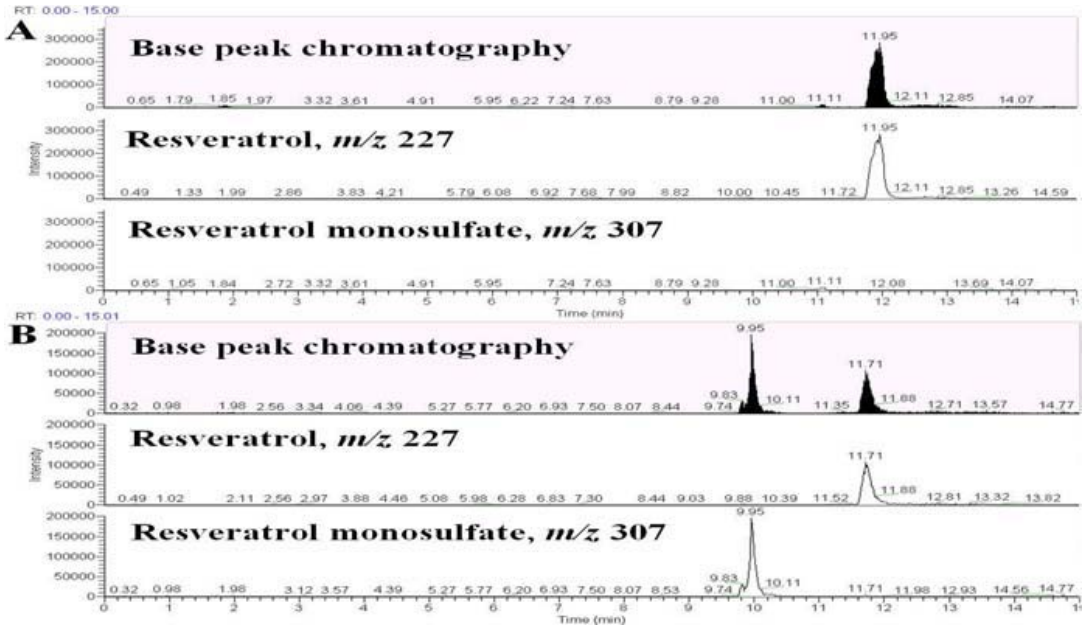

Fig. (2). APS free radical method coupled with LC tandem MS to monitor oxidative derivatives; (**A**) Not treated with APS; resveratrol monosulfate is not obsvered; (**B**) Treated with APS, resveratrol monosulfate is observed.

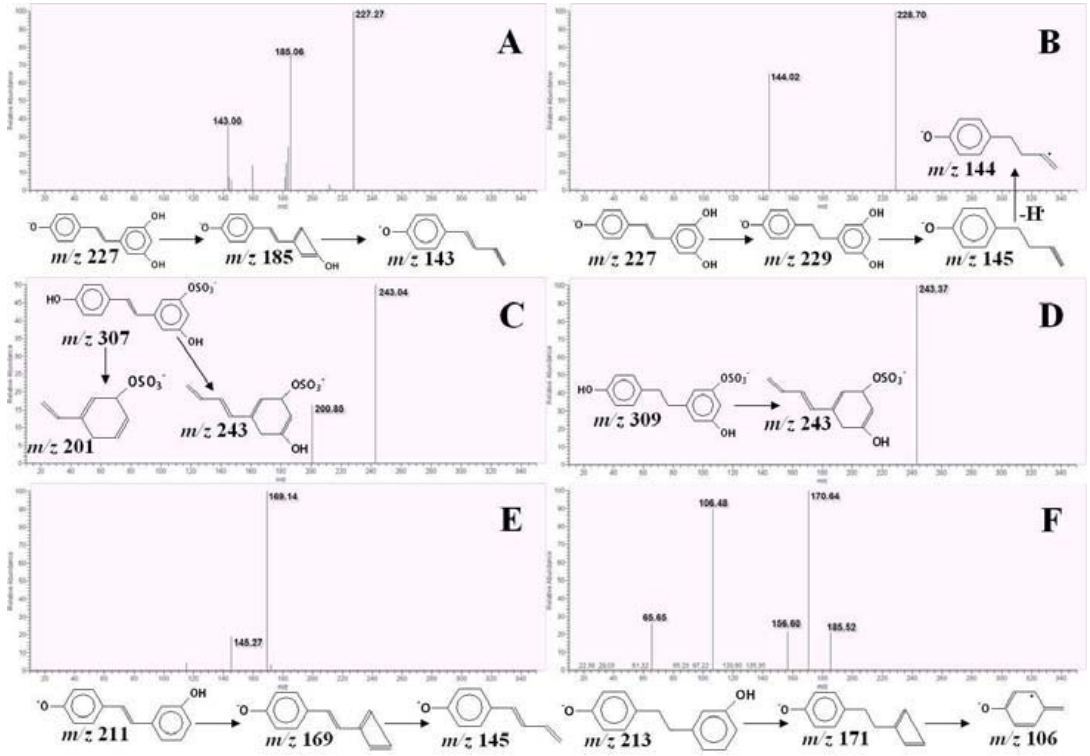

Fig. (3). MS/MS spectra of resveratrol and its derivatives with fragmented ion spectrum and proposed fragmentation pathways (**A**–**F**); resveratrol (*m/z* 227, **A**), dihydroresveratrol (*m/z* 229, **B**), resveratrol monosulfate (*m/z* 307, **C**), dihdroresveratrol monosulfate (*m/z* 309, **D**), 3,4′-dihydroxy-*trans*-stilbene (*m/z* 211, **E**), and lunularin (*m/z* 213, **F**).

m/z 227 > 143 as well as *m/z* 307 > 243 and *m/z* 307 > 201 of resveratrol monosulfate. Additionally, the conditions of the MRM scanning mode in tandem mass were setup in a negative ion mode, with 0.05 s in one transition, and collision energy was set at 23 V. Furthermore, the tune file of tandem mass was adjusted in negative mode with a tube lens offset –188 V.

MS spectra obtained from sequential sampling with the MRM scanning mode are shown in Fig. (**4**). Fig. (**4A**) (sequential sampling 00) shows the spectra for the sample where APS was not added; Fig. (**4B**) (sequential sampling 09) shows the spectra for the sample that was injected nine times after APS addition; Fig. (**4C**) (sequential sampling 19) shows the spectra for the sample injected 19 times; and

finally, Fig. (**4D**) (sequential sampling 30) shows the spectra for the sample injected 30 times. According to the sequential sampling, the changes in quantities of individual oxidative derivatives were observed. As the normalization factor was based on the quantity of resveratrol, the changes in quantities of every oxidative derivatives were followed over time. According to the bar chart shown in Fig. (**5**), the results of resveratrol metabolites changes in quantities with time can be utilized to predict the generation of individual resveratrol metabolites. According to Fig. (**5A**), resveratrol monosulfate (*m/z* 307) increased with increasing concentration, which is normalized by resveratrol (*m/z* 227). However, dihydroresveratrol monosulfate (*m/z* 309) increased for the first two hours, and steadily decreased as the reaction time progressed. In addition the concentration of dihydroresveratrol (*m/z* 229) reached a maximum after 15 min and then stabilized. Finally, 3,4′-dihydroxy-*trans*-stilbene (*m/z* 211) and lunularin (*m/z* 213) were in a random situation with low MS intensity. We considered that 3,4′-dihydroxy-*trans*-stilbene and lunularin were produced in a microenvironment with higher variations and were not detected easily.

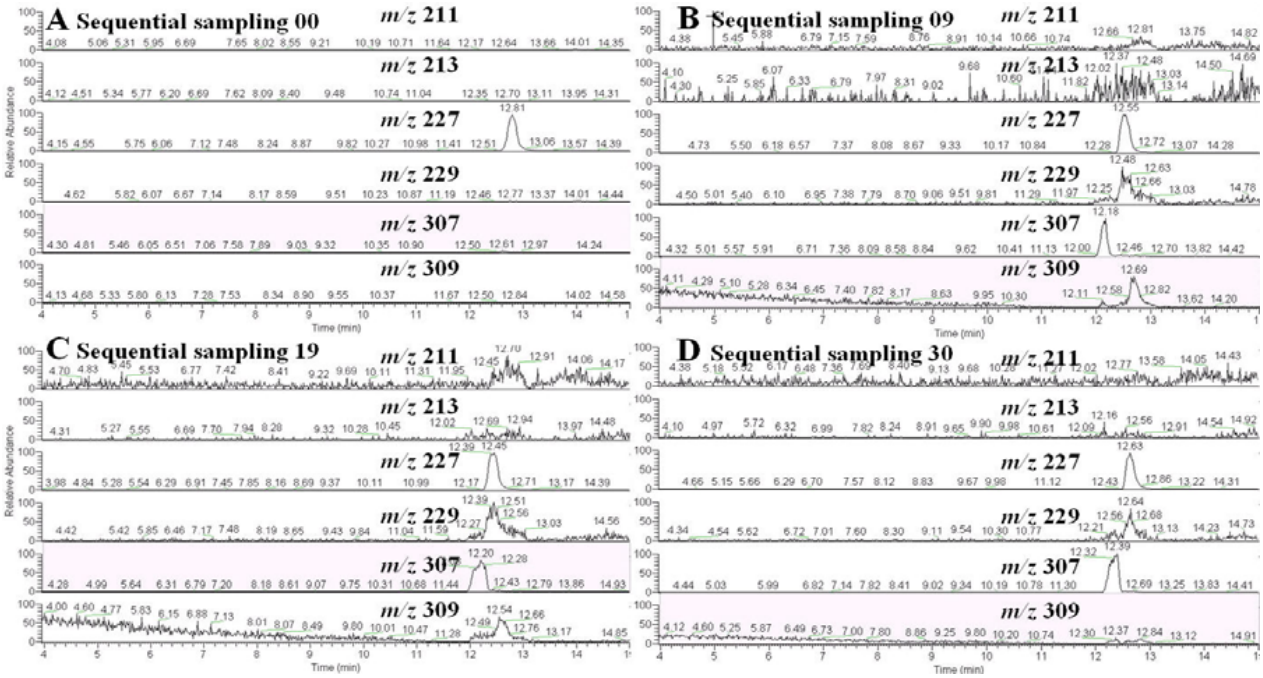

Fig. (4). Sequential analysis of resveratrol and its oxidative derivatives by tandem MS with the MRM scanning mode at sample sequence 00 (untreated with APS, **A**), sequence 09 (treated with APS, **B**), sequence 19 (treated with APS, **C**), and final sampling sequence 30 (treated with APS, **D**).

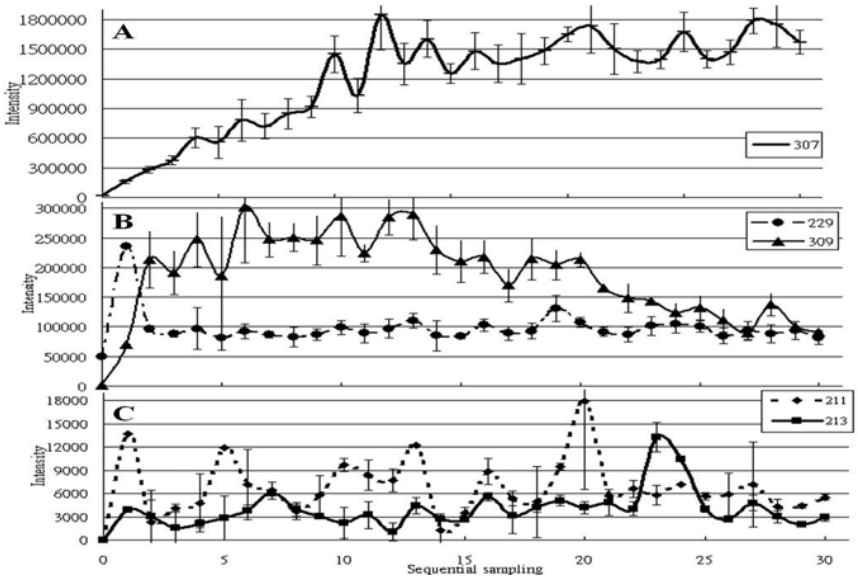

Fig. (5). Illustrated curves of normalized concentration changes in oxidative compounds as detected by MRM mode tandem MS. (**A**) resveratrol monosulfate (*m/z* 307), (**B**) dihydroresveratrol (*m/z* 229) and dihydroresveratrol monosulfate (*m/z* 309), and (**C**) 3,4′-dihydroxy-*trans*-stilbene (*m/z* 211) and lunularin (*m/z* 213).

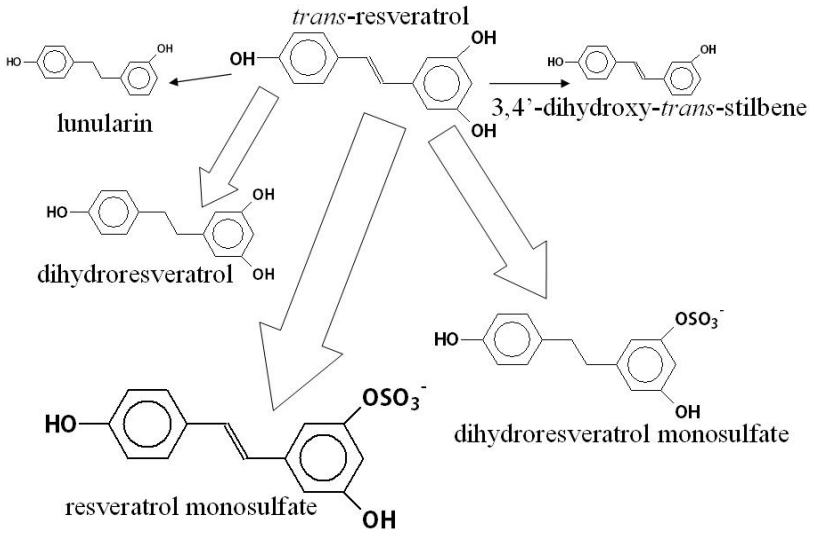

Fig. (6). Schematic representation of the proposed resveratrol metabolic pathway based on normalized concentration changes in oxidative compounds.

3.4. Pathways of Resveratrol and its Oxidative Derivatives

Based on Fig. (**5**), the prediction of resveratrol metabolic pathway was proposed. In Fig. (**6**), 3,4′-dihydroxy-*trans*-stilbene and lunularin are illustrated using smaller chemical structure which is representative of their low concentrations in the predictive metabolic pathway. Dihydroresveratrol and dihydroresveratrol monosulfate with higher concentrations are labeled with arrow marks and larger chemical structures. Finally, resveratrol monosulfate with the highest concentration is represented by the largest chemical structure.

The results show that APS generates free radicals from persulfate to attack resveratrol and produce resveratrol monosulfate. We considered this to be the key factor in obtaining resveratrol monosulfate in highest concentration of all oxidative products. However, other oxidative derivatives were observed and detected in APS free radical oxidation method.

CONCLUSION

In this study, the experiments showed that APS generates free radicals to react with resveratrol and produce its oxidative derivatives. According to the oxidative method, we can predict the metabolic pathway of resveratrol. In addition, oxidative derivatives could be continuously monitored via sequential sampling. Moreover, the free radical generated technique is a simple, well-controlled, time and labor saving, and convenient method. However, free radicals generated by APS produce compounds with APS attached, such as resveratrol monosulfate and dihydroresveratrol monosulfate. Perhaps, other oxidative methods and reagents could be utilized for metabolic prediction such as hydrogen peroxide, ozone, sodium hypochlorite, and potassium permanganate.

CONFLICT OF INTEREST

The authors confirm that this article content has no conflict of interest.

ACKNOWLEDGEMENTS

We thank the supporting funds by a grant from cooperative plans between National Sun Yat-Sen University and Kaohsiung Medical University (#NSYSUKMU 102-P029), and the National Science Council (NSC Grants NSC 102-2113-M-037-013-MY2, and NSC 102-2632-B-037-001-MY3), Taipei, Taiwan. We also thank the Center for Research Resources and Development of Kaohsiung Medical University for the supports of tandem MS.

REFERENCES

[1] Liu, D.; Zheng, X.; Tang, Y.; Zi, J.; Nan, Y.; Wang, S.; Xiao, C.; Zhu, J., Chen, C., Metabolism of tanshinol borneol ester in rat and human liver microsomes. *Drug Metab. Dispos.*, **2010**, *38*, 1464-1470.

[2] Kamikyouden, N.; Sugihara, K.; Watanabe, Y.; Uramaru, N.; Murahashi, T.; Kuroyanagi, M.; Sanoh, S.; Ohta, S.; Kitamura, S. 2,5-Dihydroxy-4-methoxybenzophenone: a novel major in vitro metabolite of benzophenone-3 formed by rat and human liver microsomes. *Xenobiotica*, **2013**, *43*, 514-519.

[3] Yamanaka, H.; Nakajima, M.; Nishimura, K.; Yoshida, R.; Fukami, T.; Katoh, M., Yokoi, T., Metabolic profile of nicotine in subjects whose CYP2A6 gene is deleted. *Eur. J. Pharm. Sci.*, **2004**, *22*, 419-425.

[4] Brandon, E.F.; Raap, C.D.; Meijerman, I.; Beijnen, J.H., Schellens, J.H. An update on in vitro test methods in human hepatic drug biotransformation research: pros and cons. *Toxicol. Appl. Pharmacol.,* **2003**, *189*, 233-246.

[5] Goyal, R.N.; Gupta, V.K.; Sangal, A.; Bachheti, N. Voltammetric determination of uric acid at a fullerene-C-60-modified glassy carbon electrode. *Electroanal.,* **2005**, *17*, 2217-2223.

[6] Habibi, B.; Pezhhan, H.; Pournaghi-Azar, M.H. Voltammetric and amperometric determination of uric acid at a carbon-ceramic electrode modified with multi walled carbon nanotubes. *Microchim. Acta,* **2010**, *169*, 313-320.

[7] Goyal, R.N.; Sangal, A. Electrochemical investigations of adenosine at solid electrodes. *J. Electroanal. Chem.,* **2002**, *521*, 72-80.

[8] Goyal, R. N.; Tyagi, A., Investigations into the electrooxidation of guanosine-5'-triphosphate at the pyrolytic graphite electrode. *Anal. Bioanal. Chem.,* **2005**, *382*, 1683-1690.

[9] Boussicault, F.; Robert, M., Electron transfer in DNA and in DNA-related biological processes. Electrochemical insights. *Chem. Rev.,* **2008**, *108*, 2622-2645.

[10] Oliveira, S.C.; Oliveira-Brett, A.M., In situ DNA oxidative damage by electrochemically generated hydroxyl free radicals on a boron-doped diamond electrode. *Langmuir,* **2012**, *28*, 4896-4901.

[11] Oliveira-Brett, A.M.; Piedade, J.A.; Silva, L.A., Diculescu, V.C., Voltammetric determination of all DNA nucleotides. *Anal. Biochem.,* **2004**, *332*, 321-329.

[12] Arteaga, J.F.; Ruiz-Montoya, M.; Palma, A.; Alonso-Garrido, G.; Pintado, S., Rodriguez-Mellado, J.M. Comparison of the simple cyclic voltammetry (CV) and DPPH assays for the determination of antioxidant capacity of active principles. *Molecules,* **2012**, *17*, 5126-5138.

[13] Volk, K.J.; Lee, M.S.; Yost, R.A.; Brajter-Toth, A. Electrochemistry/thermospray/tandem mass spectrometry in the study of biooxidation of purines. *Anal. Chem.,* **1988**, *60*, 720-722.

[14] Volk, K.J.; Yost, R.A., Brajter-Toth, A., On-line electrochemistry/ thermospray/tandem mass spectrometry as a new approach to the study of redox reactions: the oxidation of uric acid. *Anal. Chem.,* **1989**, *61*, 1709-1717.

[15] Volk, K.J.; Yost, R.A.; Brajter-Toth, A. Characterization of solution-phase and gas-phase reactions in on-line electrochemistry-thermospray tandem mass spectrometry. *J. Chromatogr.,* **1989**, *474*, 231-243.

[16] Volk, K.J.; Yost, R.A., Brajter-Toth, A. On-line mass spectrometric investigation of the peroxidase-catalysed oxidation of uric acid. *J. Pharm. Biomed. Anal.,* **1990**, *8*, 205-215.

[17] van Leeuwen, S.M.; Blankert, B.; Kauffmann, J.M.; Karst, U. Prediction of clozapine metabolism by on-line electrochemistry/ liquid chromatography/mass spectrometry. *Anal. Bioanal. Chem.,* **2005**, *382*, 742-750.

[18] Baumann, A.; Lohmann, W.; Schubert, B.; Oberacher, H., Karst, U., Metabolic studies of tetrazepam based on electrochemical a simulation in comparison to *in vivo* and *in vitro* methods. *J. Chromatogr. A.,* **2009**, *1216*, 3192-3198.

[19] Schubert, B.; Pavlic, M.; Libiseller, K., Oberacher, H., Unraveling the metabolic transformation of tetrazepam to diazepam with mass spectrometric methods. *Anal. Bioanal. Chem.,* **2008**, *392*, 1299-1308.

[20] Trumpler, S.; Lohmann, W.; Meermann, B.; Buscher, W.; Sperling, M.; Karst, U. Interaction of thimerosal with proteins-ethylmercury adduct formation of human serum albumin and beta-lactoglobulin A. *Metallomics,* **2009**, *1*, 87-91.

[21] Melles, D.; Vielhaber, T.; Baumann, A.; Zazzeroni, R.; Karst, U. Electrochemical oxidation and protein adduct formation of aniline: a liquid chromatography/mass spectrometry study. *Anal. Bioanal. Chem.,* **2012**, *403*, 377-384.

[22] Baumann, A.; Lohmann, W.; Jahn, S.; Karst, U. On-Line Electrochemistry/Electrospray Ionization Mass Spectrometry (EC/ESI-MS) for the Generation and Identification of Nucleotide Oxidation Products. *Electroanal.,* **2010**, *22*, 286-292.

[23] Zhang, Y.; Dewald, H.D., Chen, H., Online mass spectrometric analysis of proteins/peptides following electrolytic cleavage of disulfide bonds. *J. Proteome. Res.,* **2011**, *10*, 1293-1304.

[24] Bode, L.M.; Bunzel, D.; Huch, M.; Cho, G. S.; Ruhland, D.; Bunzel, M.; Bub, A.; Franz, C.M.; Kulling, S.E. *In vivo* and *in vitro* metabolism of trans-resveratrol by human gut microbiota. *Am. J. Clin. Nutr.,* **2013**, *97*, 295-309.

[25] Shu, X.H.; Li, H.; Sun, Z.; Wu, M.L.; Ma, J.X.; Wang, J.M.; Wang, Q.; Sun, Y.; Fu, Y.S.; Chen, X.Y.; Kong, Q.Y.; Liu, J. Identification of metabolic pattern and bioactive form of resveratrol in human medulloblastoma cells. *Biochem. Pharmacol.,* **2010**, *79*, 1516-1525.

[26] Liang, S. S.; Shiue, Y. L.; Kuo, C. J.; Guo, S. E.; Liao, W. T., Tsai, E. M., Online Monitoring Oxidative Products and Metabolites of Nicotine by Free Radicals Generation with Fenton Reaction in Tandem Mass Spectrometry. *Sci. World. J.,* **2013**, http://dx.doi.org/10.1155/2013/189162.

[27] Jang, M.; Cai, L.; Udeani, G.O.; Slowing, K.V.; Thomas, C.F.; Beecher, C.W.; Fong, H.H.; Farnsworth, N.R.; Kinghorn, A.D.; Mehta, R.G.; Moon, R.C.; Pezzuto, J.M. Cancer chemopreventive activity of resveratrol, a natural product derived from grapes. *Science,* **1997**, *275*, 218-220.

[28] Howitz, K.T.; Bitterman, K.J.; Cohen, H.Y.; Lamming, D.W.; Lavu, S.; Wood, J.G.; Zipkin, R.E.; Chung, P.; Kisielewski, A.; Zhang, L.L.; Scherer, B.; Sinclair, D.A. Small molecule activators of sirtuins extend Saccharomyces cerevisiae lifespan. *Nature,* **2003**, *425*, 191-196.

[29] Olas, B.; Wachowicz, B. Resveratrol and vitamin C as antioxidants in blood platelets. *Thromb Res.,* **2002**, *106*, 143-148.

[30] Shakibaei, M.; Csaki, C.; Nebrich, S.; Mobasheri, A. Resveratrol suppresses interleukin-1beta-induced inflammatory signaling and apoptosis in human articular chondrocytes: potential for use as a novel nutraceutical for the treatment of osteoarthritis. *Biochem. Pharmacol.,* **2008**, *76*, 1426-1439.

[31] Zhu, J.; Yong, W.; Wu, X.; Yu, Y.; Lv, J.; Liu, C.; Mao, X.; Zhu, Y.; Xu, K.; Han, X. Anti-inflammatory effect of resveratrol on TNF-alpha-induced MCP-1 expression in adipocytes. *Biochem. Biophys. Res. Commun.,* **2008**, *369*, 471-477.

[32] Burstein, B.; Maguy, A.; Clement, R.; Gosselin, H.; Poulin, F.; Ethier, N.; Tardif, J. C.; Hebert, T. E.; Calderone, A., Nattel, S., Effects of resveratrol (trans-3,5,4'-trihydroxystilbene) treatment on cardiac remodeling following myocardial infarction. *J. Pharmacol. Exp. Ther.,* **2007**, *323*, 916-923.

[33] Rivera, L.; Moron, R.; Zarzuelo, A., Galisteo, M., Long-term resveratrol administration reduces metabolic disturbances and lowers blood pressure in obese Zucker rats. *Biochem. Pharmacol.,* **2009**, *77*, 1053-1063.

[34] Athar, M.; Back, J.H.; Tang, X.; Kim, K.H.; Kopelovich, L.; Bickers, D.R.; Kim, A.L., Resveratrol: a review of preclinical studies for human cancer prevention. *Toxicol. Appl. Pharmacol.,* **2007**, *224*, 274-283.

[35] Hudson, T.S.; Hartle, D.K.; Hursting, S.D.; Nunez, N.P.; Wang, T. T.; Young, H.A.; Arany, P.; Green, J.E. Inhibition of prostate cancer growth by muscadine grape skin extract and resveratrol through distinct mechanisms. *Cancer Res.,* **2007**, *67*, 8396-8405.

[36] Gescher, A.J.; Steward, W.P. Relationship between mechanisms, bioavailibility, and preclinical chemopreventive efficacy of resveratrol: a conundrum. *Cancer Epidem. Biomar. Prev.,* **2003**, *12*, 953-957.

Received: April 03, 2015 Revised: May 12, 2015 Accepted: May 14, 2015